PROCEEDINGS OF THE 14TH EARSeL SYMPOSIUM
GÖTEBORG/SWEDEN/6-8 JUNE 1994

Sensors and Environmental Applications of Remote Sensing

Edited by
JAN ASKNE
Chalmers University of Technology, Göteborg, Sweden

OFFPRINT

A.A. BALKEMA/ROTTERDAM/BROOKFIELD/1995

Sensors and Environmental Applications of Remote Sensing, Askne (ed.) © 1995 Balkema, Rotterdam, ISBN 90 5410 524 0

The Near Ultraviolet Spectrometer (NUVS): A new instrument for volcanic sulphur dioxide measurements

S. Mattei, S. Panachia & V. Schena
COnsorzio per la RIcerca su Sistemi di Telesensori Avanzati (CORISTA), Naples, Italy
G. Hoover
Jet Propulsion Laboratory (JPL), Pasadena, Calif., USA

ABSTRACT: Monitoring the chemical composition and flux of volcanic eruptions is one of the prospective methods for eruptions prediction. Due to the world wide distributions of volcanoes in often inaccessible regions, and their unpredictable and hazardous natures, estimation of global volcanic SO2 production using ground-based methods is difficult. Aerospace observation can be a valuable tool for a global monitoring of volcanoes. This paper describes a miniaturized dual field of view fiber optic spectrometer system used for atmospheric and volcanological observations on board the NASA SR-71 high altitude high speed aircraft, during two preliminary engineering flights.

INTRODUCTION

The observation of the atmosphere in the ultraviolet (UV) region of the electromagnetic spectrum has been of increasing interest in the last decade due to many molecules of atmospheric interest that are active in this spectral region (O_3, SO_2, NO, CS_2, HNO_2, HNO_3, etc).
The improvement of atmospheric trasparency knowledge by means of UV remote sensing techniques plays an important role to understand the basic aspects of atmospheric and geophysical processes. In particular, remote sensing of chemical composition and flux of volcanic gas emissions provides a helpfull means to better understand volcanic phenomena. It can be considered as one of the prospective methods for eruption prediction since changes in gas chemistry or flux, such as fluctuations in SO_2 emission rate, are sensitive to the condition of magma (Menyailov 1975, Casadevall et al., 1983).

Sulfur and its compounds (e.g. S, SO_2, H_2S) are among the most environmentally active and common components of volcanic eruptions. Sulphur dioxide has been considered to be the principal precursor of stratospheric H_2SO_4 aerosols, which have been implicated in global cooling observed after past major eruptions. The SO_2 molecule has strong absorption bands in UV region, in particular at the wavelengths which are often used to measure atmospheric ozone (290÷320 nm) (figure 1).

While spacecraft observations have been able to track the emission of SO_2 from large volcanoes into the stratosphere (e.g. TOMS, MLS) (Krueger 1983, Read et al. 1993), these observations have inadequate spectral and spatial resolution to satisfy the needs of vulcanologists.

In the last two years CORISTA and JPL have focused their attention on the identification of the characteristics and performance of a high resolution imaging spectrometer to be flown on board an Earth Probe class polar orbit satellite dedicated to volcanic phenomena monitoring, including the detection and tracking of SO_2 emissions from volcanic eruptions world-wide.

As a first step, a new compact airborne fiber optic spectrometer was built, able to perform simultaneous upward and downward observations.

This paper is intended to describe its preliminary test-flights aboard the high-performance NASA SR-71 research aircraft.

2 INSTRUMENT DESCRIPTION

The Near Ultraviolet Spectrometer (NUVS) consists of two miniaturized fiber optic spectrometers. It is a modular, low cost, low power consumption instrument. The use of optical fibers to collect radiation into the spectrometers greatly simplifies the mechanical layout of the instruments and permits modular development of the sensor. This

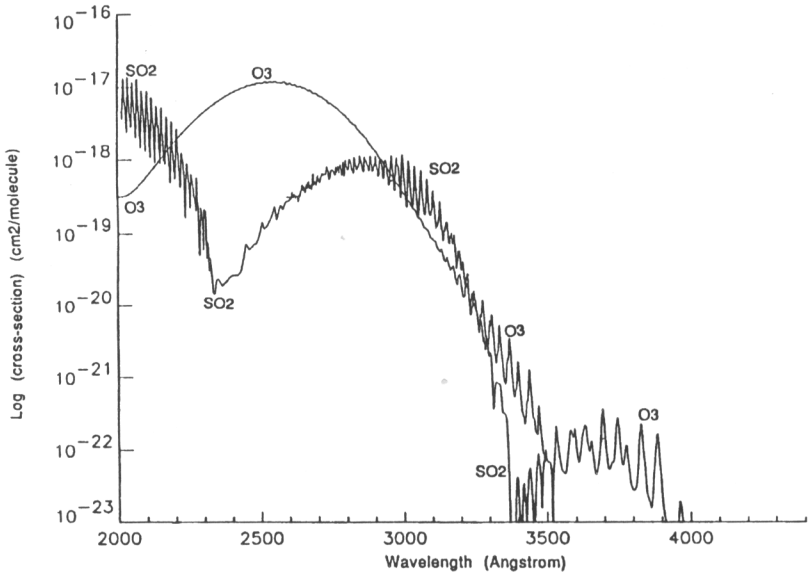

Figure 1: SO_2 and O_3 cross sections

allows the various subsystems (spectrometers, fore optics etc.) to be developed, aligned and tested independently of each other.

Figure 2 shows the instrument configuration adopted for the two engineering test flights on board the NASA SR71 aircraft. The system was assembled and hard-mounted in a little aluminium case (40×25× 20 cm). Each small spectrometer (6.7×4.6×2 cm) accepts light from a single fiber, terminated with a standard SMA connector, and disperses it across a CCD linear array (NEC μPD3575) with 1024 photosensitive elements. Some of them have been obscured to give information on the dark current during the flights, since the instrument was not equipped with a shutter. The two analog video signals coming out from the focal plane detectors are digitized by a 12 bits analog to digital converter (ADC). The entire system is operated by a 80386/25MHz microprocessor. The acquired spectra, as well as the operating programs, are

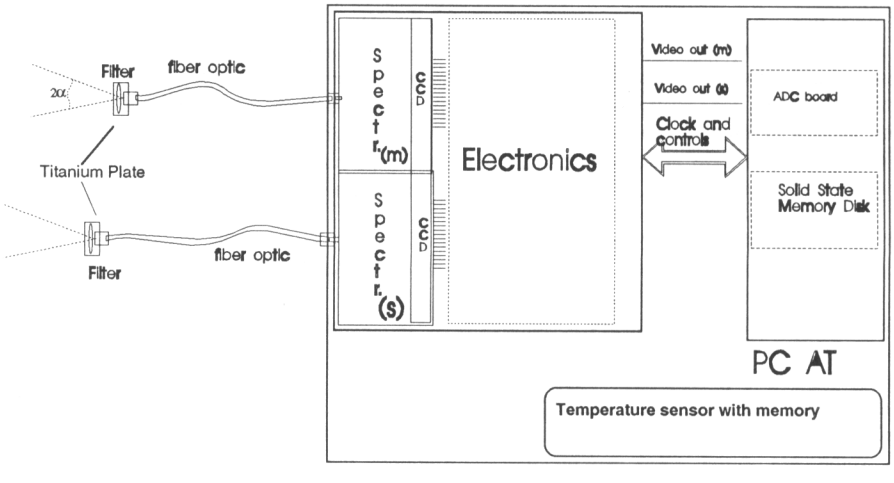

Figure2: high level block diagram of NUVS

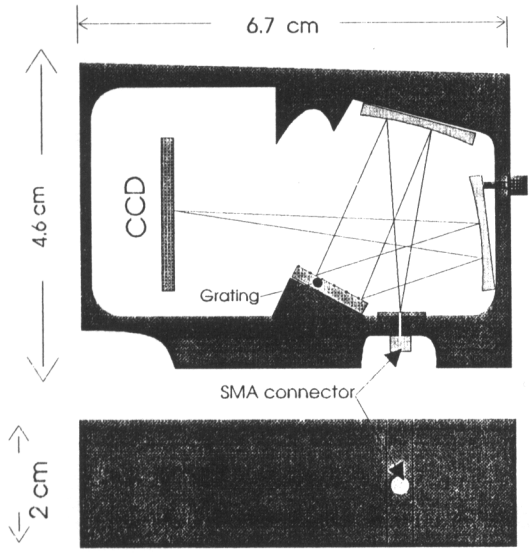

Figure 3: spectrometer optical layout

recorded in binary form on a solid state memory disk with a capacity of 8 Mbyte, that guarantees the system to operate in a non pressurized environment. A temperature sensor measures and registers the temperature of the system at regular interval of time during the flights in order to allow a reconstruction of "simulated" dark current by means of a set of temperature dependent multipliers determined by laboratory thermal characterization measurements of the system.

The spectrometers were each equipped with 2400 l/mm holographic gratings and UV grade silica fibers with 100 μm core diameter and polyimide buffer. The spectral bandpass was 250-365 nm, limited to 270-335 by interferential filters used to reduce stray light. The measured spectral resolution was ≈1.5 nm (Full Width Half Maximum, FWHM). The Instantaneous Field of View (IFOV) of each sensor was 25°, determined by the Numerical Aperture (NA=0.22) of the fibers. Therefore, for an aircraft flight altitude of 26 Km the GIFOV (Ground Instantaneous Field Of View) is a circle with a diameter of ≈11.7 km. It a cruise speed of 1 Km/sec, two subsequent GIFOV are about 50% superimposed.

3 SR71 DESCRIPTION AND ON-BOARD INSTRUMENT SET UP

The SR-71, built by Lockheed, is a long range, two places aircraft, powered by two Pratt and Whitney J58 turbojet engines. It is, for sustained flight, the highest flying, fastest aircraft in the world today. No other aircraft comes even remotely close to matching its performance for cruise flight at altitudes of 26 Km, at speeds of Mach 3 plus. The use of the SR-71 permits, among other things, a realistic simulation of the orbital observational environment with respect to SO_2 and O_3 (it flies above the zone, 20-25 Km, of highest ozone concentrations).

The SR-71 has a range of about 5550 km, without mid-air refuelling and virtually unlimited range with refuelling. Payloads can be carried internally in the mission equipment bays, located within the fuselage chines, in a small compartment (C-bay) forward of the nose wheel well, and in the detachable nose section.

Owing to its peculiar characteristics, small dimensions, fiber optic design and low power consumption, NUVS can be easily accommodated on the SR-71 airplane. Because of the operational requirements, the instrument was mounted in the C-bay, since from there it is not difficult for the fiber optical cables to reach the bottom and the top of the aircraft. Two little holes (about 5 mm diameter) were made in the skin of the aircraft to allow the mounting of two special titanium plates, with female SMA connector shape on one side, to house the blocking filters and fasten the terminal connectors (SMA connectors) of the fibers. The plates were tilted 6° to compensate for the angle of attack of the SR-71 in order to perform nadir observations. Figure 4 shows the geometry of the observation. An ON/OFF switch, to start and stop acquisition, was mounted in the aft cockpit.

The instrument flight configuration was characterized by an integration time of 2048 ms, an 6 sec time interval between two subsequent acquisitions, and an ADC (12 bits) dynamic range of 0-5 V.

The possibility of performing simultaneous upward and downward observations at altitudes above 20 Km, is very useful to analyze and separate the contributions of tropospheric and stratospheric gases (e.g. O_3).

4 LABORATORY CALIBRATIONS AND PRE AND POST-FLIGHT CHECKS

4.1 *Spectral calibration*

The dispersion relation, i.e. the wavelength λ(p) associated to each pixel p of the array, was

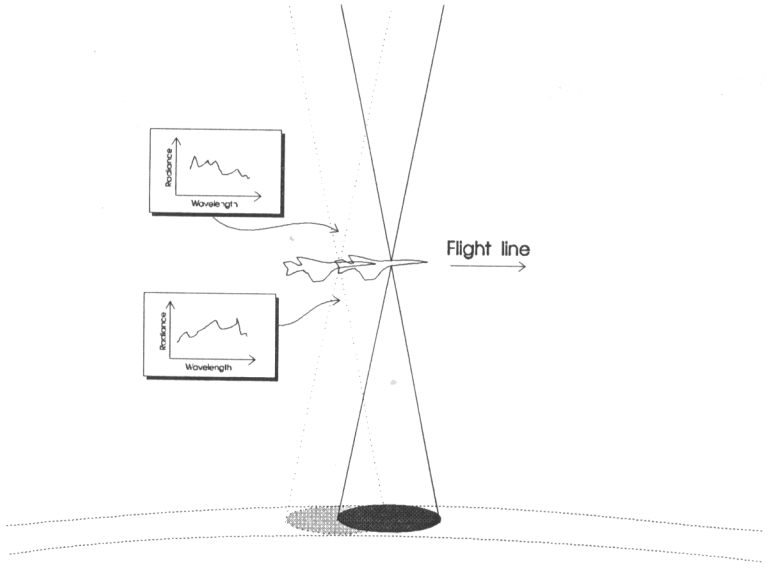

Figure 4: geometry of observation

determined using a Hg low pressure gas lamp as emitter of known spectral lines. Then a nonlinear least square fit procedure was performed to determine the coefficients of the polynomial

$$\lambda(p) = ap^2 + bp + c \qquad (1)$$

that gives the appropriate dispersion law of the system. Table 1 reportes the a, b, c values calculated for the spectrometers.

Table 1: coefficients of the dispersion relation polynomial.

	a	b	c
uplooking spectrometer	-22×10^{-6} $\pm2\times10^{-6}$	0.143± 0.003	239.9±0.7
downlooking spectrometer	-23×10^{-6} $\pm3.\times10^{-6}$	0.147± 0.003	245.1±0.7

The spectral resolution (FWHM) was measured in ≈ 1.5 nm for the flight configuration.

The spectrometers were also characterized by measuring and calculating the Optical Modulation Transfer Function (OMTF) and the MTF associated with the focal plane array calculated from its geometrical characteristics (Young 1992). The optical MTF (Slater 1980, Young 1992) was found to be dominant, i.e.

$MTF_{optical} \times MTF_{detectors} \approx MTF_{optical}$

as shown by figure 5.

This means that the focal plane is "oversampled" by the detectors array as we can see from figure 6 where it is reported an Hg vapor lamp spectral line acquired by the downlooking spectrometer.

Due to the narrow width of the lines emitted by these type of lamps, the light intensity distribution can be considered the Impulse Spectral Response Function of the spectrometer and its FWHM is then an index of its spectral resolution. The continuos line in figure 6 is the plot of the function:

$$y(\lambda)=A\,|\,2*J_1(z)/z\,|\,2+C \qquad (2)$$

where J_1 is the first order Bessel function and $z=\pi/d(\lambda-\lambda_m)$.

This function is the one that best fits, in the sense of minimum squares, the distribution of the intensity in the focal plane produced by spectral line in input. The parameters d, λ_m, and C have been estimated by a non linear least squares fit. This fact suggests the possibility of grouping the pixels to form wider spectral channels to improve the SNR without reducing the spectral resolution of the systems as well as to use a different focal plane array reducing the data to be recorded during the flight.

The procedures above described were repeated after each flights, and produced within the experimental error, the same results. The sensor showed a very good stability.

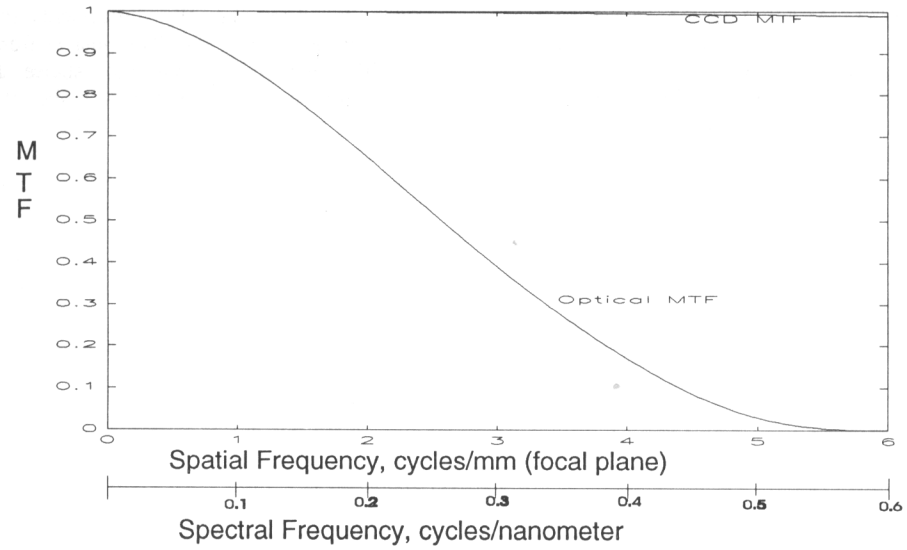

Figure 5: optical and array MTF

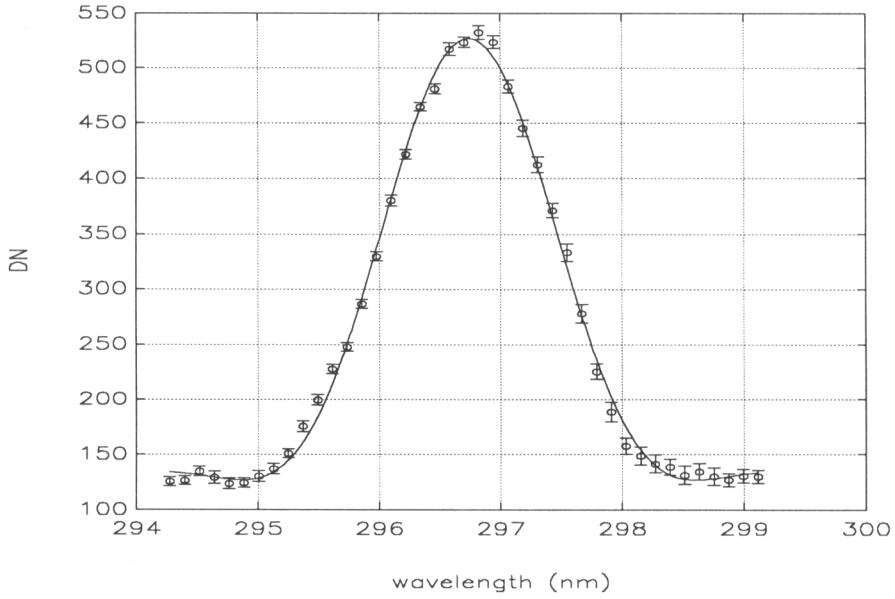

Figure 6: response of the spectrometer to a Hg spectral line

4.2 *Radiometric calibration*

The fundamental aim of the radiometric calibration is to determine a table of multipliers, MULT(λ), that, applied to the acquired data, equalizes the spectrum and converts the raw instrument data (digital numbers) to radiance values. If L(λ) is a reference known radiance in input at our sensor, then the multipliers are given by:

$$MULT(\lambda)=L(\lambda)/(DN(\lambda)-DARK(\lambda)) \quad (3)$$

where (DN(λ)-DARK(λ)) is the sensor response corrected by the dark current. In the above relation a linear response of the detectors is assumed. With our instrumentation it was not possible to perform an absolute radiometric calibration. However, it was possible to determine the instruments transfer function by positioning the fibers just in front of a stable UV lamp and varying the distance. It was found that the response is linear within 5%

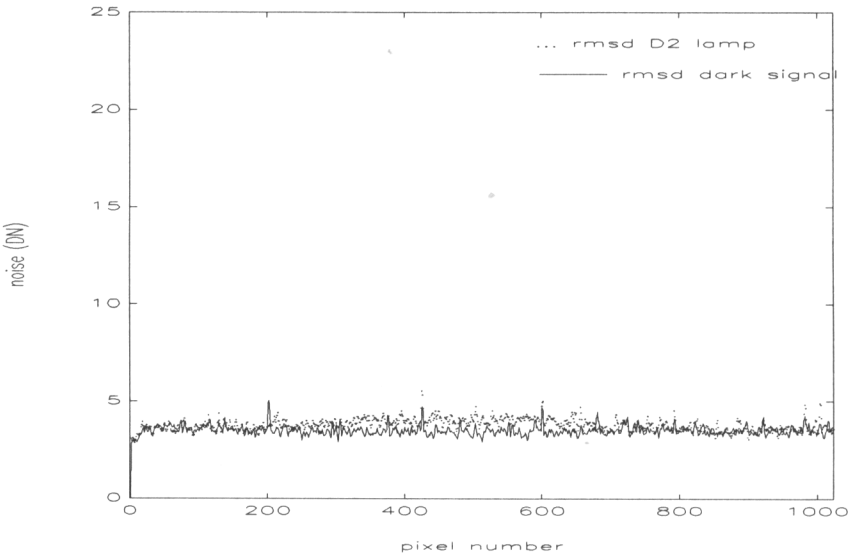

Figure 7: Measured noise (digital number)

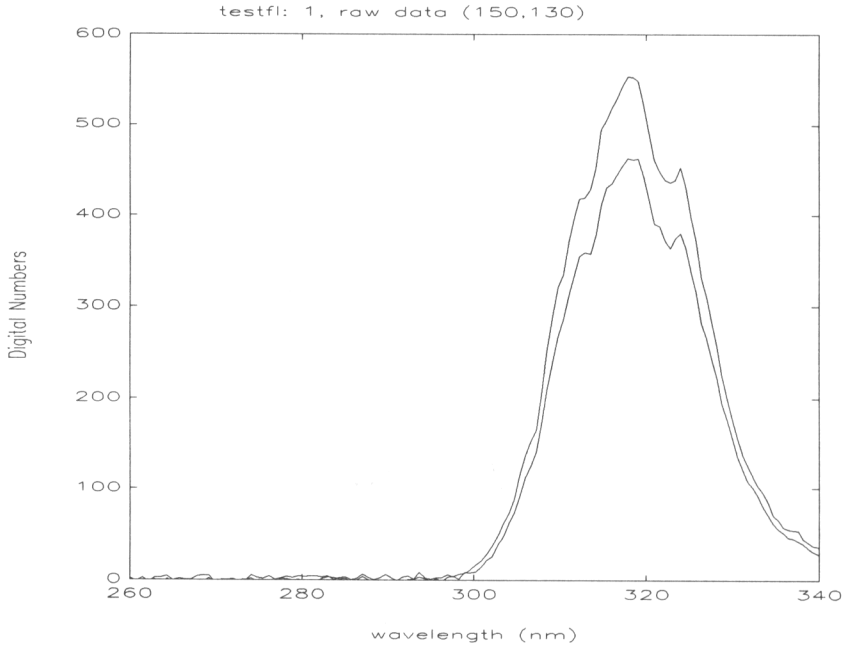

Figure 8: two spectra acquired (down-looking) from an altitude of ≈22 Km

4.3 *Thermal tests*

Thermal test of NUVS instrument was performed in the -10° to +40° C temperature using a thermal chamber made by BEMCO. A set of dark current measurements at different temperature were acquired. From them, we determined a set of temperature dependent multipliers, DM(T,i), to "reconstruct" the dark current during the flights using the count of a obscured pixel (e.g. #5) according to the relation

DARK(T,i)=c(5)*DM(T,i)

where c(5) is the count (Digital Number) of the obscured pixel in a scan during the flight, T is the temperature measured by the temperature sensor in the metallic box during the scan, i is the index (1-1024) of the pixel.

4.4 *Noise*

Noise has been calculated as the Root Mean Square Deviation (RMSD) of a sample of 50 spectra measured from a stabilized irradiance source. The conditions and operating parameters of the instrument during the measurements were set to be as close as possible to the flight ones. Figure 7 shows, for one of the spectrometers, the measured noise. In the figure is also reported the RMSD calculated with the lamp obscured.

As the arrays work far below their saturation levels, the two methods for noise calculations give similar results.

5 RESULTS OF TEST FLIGHTS

The principal objectives of our engineering test flights were essentially to verify the correct working of the sensor during the hypersonic and high altitude (≥22 Km) flights; to acquire a first set of flight data for a better definition of the operating parameters to be used in the next flights, such as integration time, dynamic range, etc; to check the resistance of the system to mechanical stress, especially during the take off and landing of the SR-71; to check the immunity of the system to the e.m. interference due to the other on-board electronics systems.

The test flights took place on 15/7/93 and on 28/7/93 with take off at 8 a.m. from Edwards Air Force Base.

During the flights the sensor worked as expected.

Moreover the pre and post flight checks have confirmed a good mechanical stability of the sensor. The spectral calibration and the radiometric sensitivity were conserved within the errors.

Figure 8 shows, as an example, two raw spectra acquired during the first flight at an altitude of about 22 km. They have been corrected for the dark current using the procedure explained in the previous paragraphs. Each five pixels were grouped to form a single wider spectral channel to improve ($\approx 5^{1/2}$) the SNR without reducing the spectral resolution.

The measured temperature inside the sensor was about 17° Celsius with little oscillation (±1°) during the whole period of the acquisition.

6 CONCLUSION

Main objective of this research program is to design an advanced high resolution very compact spectrometer system for ultraviolet atmospheric observations to be flown on board a free flying satellite.

In this framework the first step was the realization of a prototype of a miniaturized modular fiber optic, dual field of view, spectrometer system. This sensor had been tested with two engineering test flights on board the SR-71 high altitude hypersonic NASA aircraft. The engineering flights had been performed to check the correct working of the prototype system aboard the aircraft and explore the signal to noise ratio regimes for high altitude (>22Km) ultraviolet observations. The results have been satisfactory. The system worked as "expected". The miniature size and fibre optic design have proved to be fundamental for an easy installation on board the SR71. In particular only the use of optical fibres to bring the collected radiation to the spectrometers has permitted reaching the top of the aircraft from the C-bay, thus allowing simultaneous upward and downward acquisitions.

Further research is necessary to improve the system and perform reliable atmospheric high altitude UV observations. First of all a radiometric absolute radiance calibration of the system and the following hardware modifications:

- a shutter to acquire dark scans for a more accurate subtraction of the corresponding current during the flights;
- stabilization of the temperature and possibly cooling of the detectors;
- auxiliary visible cameras, synchronized with the spectrometers scans, to get imaging of the observed scenes;
- a spectral lines emitter to check the spectral calibration during the flight;

- a dedicated microcontroller to manage the system.

The use of additional fore-optics is under evaluation.

After these improvements, other high altitude flights will be performed in order to carry out a quantitative analysis on the acquired data and test atmospheric models and atmospheric inversion methods in the UV region.

At the same time it is being developed a first design of a high resolution spectrometer system to be flown aboard a free flying micro-satellite. The data acquired will integrate those of existing space-borne UV spectrometer systems, as well as those of future sensors such as Gome.

REFERENCES

Menyailov, I.A. 1975. Prediction of eruptions using changes in composition of volcanic gases. *JGR*. 39:112-125

Casadevall, T.J., Rose W., Gerlach T., Greenland L.P., Ewart J., Wundermann R. and Symonds R. 1983. Gas emissions and eruptions of Mount St. Helens through 1982. *Science*. 221:1383-1385

Krueger A.J. 1983. Sighting of El Chichon Sulphur Dioxide Clouds with the Nimbus 7 Total Ozone Mapping Spectrometer. *Science*. 220:1377-1379

Read W. G., Froidevaux L., Waters J. W. 1993. Microwave Limb Sounder (MLS) Measurements of SO_2 from Mt. Pinatubo Volcano". *sub. to Geophysical Research Letters*

Young M. 1992. *Optics and laser*. Berlin: Springer Verlag:

Slater N.S. 1980. *Remote sensing: Optics and Optical Systems*. London: Addison-Wesley Publishing Company